

Non-classicality tests with entangled coherent states

G. Torlai¹, G. McKeown², P. Marek³, R. Filip³, G. De Chiara²,
M. G. A. Paris⁴, F. L. Semiao⁵, H. Jeong⁶, and M. Paternostro¹

¹*Department of Physics, Ludwig Maximilians Universität, Schellingstraße 4 80799, Munich, Germany*

²*Centre for Theoretical Atomic, Molecular and Optical Physics,*

School of Mathematics and Physics, Queen's University, Belfast BT7 1NN, United Kingdom

³*Department of Optics, Palacký University, 17. listopadu 1192/12, 77207 Olomouc, Czech Republic*

⁴*Dipartimento di Fisica, Università degli Studi di Milano, I-20133 Milano, Italy*

⁵*Centro de Ciências Naturais e Humanas, Universidade Federal do ABC, 09210-170, Santo André, São Paulo, Brazil and*

⁶*Center for Macroscopic Quantum Control, Department of Physics and Astronomy,
Seoul National University, Seoul, 151-742, Korea*

We review part of the body of work developed on the use of entangled coherent states (ECSs) and their generalization in the performance of non-classicality tests such as Bell inequalities (including their multipartite versions) and single-party contextuality inequalities. We show that a self-contained programme of investigations along such lines is indeed possible and rather successful when local operations based on the combination of both linear and non-linear bosonic operations and dichotomized homodyne measurements are used over ECS-like states. Moreover, we discuss the improvements that may arise from the use of noiseless local amplifiers over the modes participating to a given ECS-like state, thus providing an interesting forward look of experimental relevance.

Besides embodying useful resources for quantum computation and information [1], entangled coherent states (ECSs) are interesting testbed states for the addressing of fundamental questions related to the contrast between quantum and classical mechanics. As a significant example, it is worth mentioning that the non-local nature of an ECS has been extensively studied in the past [2–7]. A number of approaches has been used for the falsification of Bell-CHSH inequalities [8] by either ECSs or their generalisation [9]. In this manuscript, we review recent efforts made along the lines of building up a self-consistent and contained programme for the assessment of non-classicality via ECSs and their extensions/generalizations in various directions, including the multipartite scenario. We concentrate our attention to the framework based on the use of effective local rotations and homodyne measurements, which have been proven useful for the violation of Bell-CHSH inequalities [5–7].

In this context, we discuss a recently proposed test of local realism for ECSs having an arbitrarily small amplitude, supplemented by the application of local noiseless amplification to the components of the system [10, 11]. Needless to say, the non-deterministic nature of local amplification operations requires postselection of measurement outcomes and the invocation of the fair-sampling assumption, which we consider valid throughout our study. By increasing the amplitude of a coherent-state component without amplifying the quantum fluctuations, we show that the maximal violation of the Bell inequality can be approached. The threshold for the violation of the CHSH inequality can be considerably lowered, thus realising the mechanism sought above. We then move to the case of multipartite quantum correlations shared by systems that, when individually taken, are fully classical and revealed by instruments far from offering any single-quantum resolution. We address the case of multipartite GHZ-like entanglement shared by

bosonic systems that are locally prepared in thermal states [7] and demonstrate that they violate properly designed Bell-like nonlocality inequalities up to the maximum value allowed for a given representative of such class of states. Similar conclusions can be drawn for W-like states. Finally, we use the general tools designed for ECS-based Bell tests to show that they are fit to prove the state-independent incompatibility of quantum mechanics and non-contextual arguments as embodied by the Kochen-Specker theorem [12–14]. We use the same inequality as in Ref. [15], which is constructed by means of the effective bidimensional observables that we also exploit for the Bell-CHSH inequalities mentioned above. While, on one hand, the number of observables necessary for our task is strictly the same as for discrete-variable systems, our proposal may pave the way to a foreseeable experimental implementation faithful to the constraint of context independence.

I. RESOURCE STATE AND TOOLS

In this Section we formally introduce the class of states used in our analysis together with the formalism and tools necessary for the measurements required by our tests of nonclassicality. Although bosonic modes of any nature could be used to realize our proposal, it is natural to consider hereafter ECSs of optical field modes. Among the states falling into the family of ECSs, we consider

$$|\text{ECS}(\alpha)\rangle_{AB} = \frac{|\alpha, \alpha\rangle_{AB} + |-\alpha, -\alpha\rangle_{AB}}{\sqrt{2(1 + e^{-4|\alpha|^2})}}, \quad (1)$$

where $|\alpha\rangle_j = \hat{D}_j(\alpha)|0\rangle_j$ is a coherent state of amplitude $\alpha \in \mathbb{C}$, $\hat{D}_j(\alpha) = \exp[\alpha\hat{a}_j^\dagger - \alpha^*\hat{a}_j]$ is the displacement operator, $|0\rangle_j$ is the vacuum state of field mode $j = A, B$ with associated creation (annihilation) operator \hat{a}_j^\dagger (\hat{a}_j).

In this Section, for easiness of calculation and without affecting the generality of our discussions, we consider only the case of $\alpha \in \mathbb{R}$. The generalisation of Eq. (1) to the multipartite case will be addressed in details in Sec. III.

In general, the tests studied in this manuscript will require the distribution of state (1) [or its generalisations] to remote agents having the task of performing local effective rotations and measurements. Here we thus describe the class of local operations that we will consider and provide their physical embodiments. We consider the transformation $\mathbf{v}_j \rightarrow \hat{R}(\theta_j, \varphi_j)\mathbf{v}_j$ over the vector $\mathbf{v}_j = (|\alpha\rangle_j \quad |-\alpha\rangle_j)^t$ for mode j with

$$\hat{R}(\theta_j, \varphi_j) = \begin{pmatrix} \sin \frac{\theta_j}{2} & e^{i\varphi_j} \cos \frac{\theta_j}{2} \\ e^{-i\varphi_j} \cos \frac{\theta_j}{2} & -\sin \frac{\theta_j}{2} \end{pmatrix}. \quad (2)$$

The 2×2 matrix describing such rotation in the space spanned by $\{|\alpha\rangle, |-\alpha\rangle\}$ can be decomposed into the sequence of elementary rotations $\mathcal{U}_z(-\varphi_j/2)\mathcal{U}_x(\pi/4)\mathcal{U}_z(\vartheta_j/2)\mathcal{U}_x(\pi/4)\mathcal{U}_z(\varphi_j/2)$ with $\mathcal{U}_{x,z}(\xi) = e^{i\xi\sigma_{x,z}}$ and where σ_k is the k -Pauli matrix ($k = x, y, z$). The effect of $\mathcal{U}_z(\xi)$ on a coherent state $|\alpha\rangle$ can be effectively approximated by a phase-space displacement operation $\hat{D}(i\xi/2\alpha)$, while $\mathcal{U}_x(\pi/4)$ can be implemented using the Kerr-like single-mode nonlinearity $U_{NL} = e^{-i\pi(\hat{a}^\dagger\hat{a})^2/2}$. The physical implementation of Eqs. (2) would thus be given by the sequence [5, 6]

$$\hat{R}(\theta_j, \varphi_j) = \hat{D}_j(-i\varphi_j/4\alpha)\hat{U}_{NL}\hat{D}_j(i\theta_j/4\alpha)\hat{U}_{NL}\hat{D}_j(i\varphi_j/4\alpha). \quad (3)$$

After a lengthy but straightforward calculation, one gathers the explicit transformation experienced by $|\pm\alpha\rangle_j$, which can be cast into the form

$$\begin{aligned} |\alpha\rangle_j &\rightarrow \frac{1}{2} \left\{ e^{i\frac{\theta_j}{4}} \left[|\alpha + \frac{i\theta_j}{4\alpha}\rangle + ie^{i\frac{\varphi_j}{2}} |-\alpha - \frac{i\varphi_j}{2\alpha} - \frac{i\theta_j}{4\alpha}\rangle \right] \right. \\ &\quad \left. + ie^{-i\frac{\theta_j}{4}} \left[e^{i\frac{\varphi_j}{2}} |-\alpha - \frac{i\varphi_j}{2\alpha} + \frac{i\theta_j}{4\alpha}\rangle + i|\alpha - \frac{i\theta_j}{4\alpha}\rangle \right] \right\}, \\ |-\alpha\rangle_j &\rightarrow \frac{1}{2} \left\{ ie^{i\frac{\theta_j}{4}} \left[i|-\alpha - \frac{i\theta_j}{4\alpha}\rangle + e^{-i\frac{\varphi_j}{2}} |\alpha - \frac{i\varphi_j}{2\alpha} + \frac{i\theta_j}{4\alpha}\rangle \right] \right. \\ &\quad \left. + e^{-i\frac{\theta_j}{4}} \left[ie^{-i\frac{\varphi_j}{2}} |\alpha - \frac{i\varphi_j}{2\alpha} - \frac{i\theta_j}{4\alpha}\rangle + |-\alpha + \frac{i\theta_j}{4\alpha}\rangle \right] \right\}. \end{aligned} \quad (4)$$

For most of the tests that will be run throughout this paper require the performance of dichotomic measurements on the locally rotated state of a field mode. Our framework will make use of experimentally non-demanding and highly efficient homodyne measurements, which we take here as projections onto the in-phase quadrature eigenstate $|x\rangle$. We can thus determine the joint probability-amplitude function

$$C(\{\theta\}, \{\varphi\}, x, y) = {}_{AB} \langle x, y | \hat{R}(\theta_A, \varphi_A) \hat{R}(\theta_B, \varphi_B) | \text{ECS} \rangle_{AB}, \quad (5)$$

where $\{\theta\} \equiv \{\theta_A, \theta_B\}$ and $\{\varphi\} = \{\varphi_A, \varphi_B\}$ identify the two sets of relevant angles. A dichotomic variable is then

constructed by assigning value $+1$ to the outcome of a homodyne measurement such that $x \geq 0$ and -1 otherwise. The corresponding joint probability is

$$P_{kl}(\{\theta\}, \{\varphi\}) = \int_{\omega_k} dx \int_{\omega_l} dy |C(\{\theta\}, \{\varphi\}, x, y)|^2, \quad (6)$$

where $k, l = \pm$, $\omega_+ = [0, +\infty]$, and $\omega_- = [-\infty, 0]$. We can now introduce the correlation function

$$\mathcal{C}(\{\theta\}, \{\varphi\}) = \sum_{k,l=\pm} P_{kk}(\{\theta\}, \{\varphi\}) - \sum_{k \neq l=\pm} P_{kl}(\{\theta\}, \{\varphi\}). \quad (7)$$

II. BELL-CHSH INEQUALITY WITH LOCALLY AMPLIFIED ECS

Following the proposal put forward in Ref. [5–7], the non local nature of ECSs can be tested by means of th-elocal operations described above and dichotomized homodyne measurements. An analysis of the behavior of the Bell-CHSH function associated with such operating conditions can be found in Refs. [5, 6], where it is shown that the bound imposed by local realistic theories can be violated by an ECS with $\alpha \gtrsim 1$ and entangled thermal states (ETSS) displaced by a sufficiently large amount.

In Ref. [16] we have modifies such scheme by introducing local amplification stages as shown in Fig. 1, considering the local transformations

$$\hat{U}_j = \hat{G}_j \hat{R}_j(\theta_j, 0) \quad (j = A, B) \quad (8)$$

We have introduced the local noiseless amplification described by the operator $\hat{G}_j = \exp[(g-1)\hat{a}_j^\dagger\hat{a}_j]$ [17], where $g \geq 1$ is the gain of the amplifier. For now, we retain the full form of the amplification operator to illustrate the working principle of our proposal. Moreover, in full agreement with standard Bell-CHSH inequality tests, we set $\varphi_j = 0$ throughout this Section, which is sufficient to violate the local realistic bound.

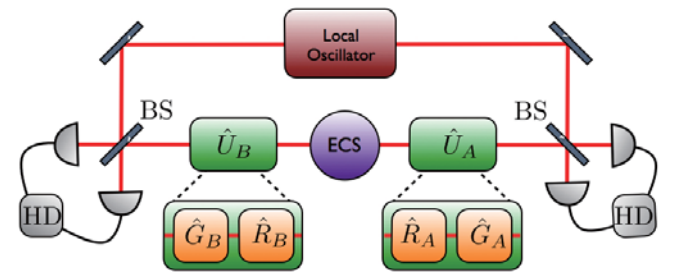


FIG. 1. Scheme for the violation of the CHSH inequality with amplified entangled coherent state. We show the source of ECS states, the local oscillator (LO) needed for homodyne measurements, and the decomposition of the local unitary transformations \hat{U}_j given in terms of the rotations $\hat{R}(\theta_j)$ and local amplification \hat{G}_j ($j = A, B$). We also show the symbols for beamsplitters and homodyners.

In what follows, we will retain only the cases where bilateral local amplification is successfully performed. Let us consider the effect of $\hat{U}_A \otimes \hat{U}_B$ on $|\text{ECS}(\alpha)\rangle$. As $\hat{G}_j |\alpha\rangle_j = |\tilde{\alpha}\rangle_j$ with $\tilde{\alpha} = \alpha e^{g-1}$, it is straightforward to show that

$$\begin{aligned} |\psi_f\rangle &= \mathcal{N}(\hat{U}_A \otimes \hat{U}_B) |\text{ECS}(\alpha)\rangle \\ &= \mathcal{N} \{ \cos[\theta_B - \theta_A] |\text{ECS}(\tilde{\alpha})\rangle + \sin[\theta_B - \theta_A] |\text{ECS}'(\tilde{\alpha})\rangle \} \end{aligned} \quad (9)$$

with $\mathcal{N} = 1/(2+2\cos[\theta_A - \theta_B]e^{-4\tilde{\alpha}^2})^{1/2}$, $\nu = \cos[\theta_A - \theta_B]$, and where we have introduced the unnormalized ECS $|\text{ECS}'(\alpha)\rangle = |\alpha, -\alpha\rangle_{AB} - |-\alpha, \alpha\rangle_{AB}$. Eq. (9) has the very same structure that would be taken using $|\text{ECS}(\alpha)\rangle$, bi-local rotation and no amplification [5], the only change being the actual amplitude of the coherent-state components. In turn, this implies that, upon application of the proposal for Bell-CHSH test discussed in [5–7] we get the following expression for the correlation function between measurement outcomes following the rotation of the modes' state by θ_A and θ_B respectively

$$\mathcal{C}_{\tilde{\alpha}}(\theta_A, \theta_B, 0, 0) = \frac{\text{Erf}^2[\sqrt{2}\tilde{\alpha}]}{1 + \nu e^{-4\tilde{\alpha}^2}} \cos[\theta_A - \theta_B] \quad (10)$$

with $\text{Erf}[\cdot]$ the Error function. The Bell-CHSH inequality that we should consider is thus written as

$$|\mathcal{B}(\tilde{\alpha}, \Theta)| = |\mathcal{C}_{\tilde{\alpha}}(\theta_{A1}, \theta_{B1}, 0, 0) + \mathcal{C}_{\tilde{\alpha}}(\theta_{A1}, \theta_{B2}, 0, 0) + \mathcal{C}_{\tilde{\alpha}}(\theta_{A2}, \theta_{B1}, 0, 0) - \mathcal{C}_{\tilde{\alpha}}(\theta_{A2}, \theta_{B2}, 0, 0)| \leq 2, \quad (11)$$

where $\Theta = \{\theta_{A1}, \theta_{A2}, \theta_{B1}, \theta_{B2}\}$ is a set of rotations angles. Quantum mechanically, this inequality can be violated using ECSs, the set of rotations in Eq. (2) and dichotomic homodyne detection. By calling $\bar{\alpha}$ the amplitude of the coherent-state components at which the Bell-CHSH inequality is first violated and preparing $|\text{ECS}_+(\alpha_a)\rangle$ with $\alpha_a \ll \bar{\alpha}$, we can get $|\mathcal{B}| > 2$ using a gain such that

$$g \geq 1 + \ln(\bar{\alpha}/\alpha_a). \quad (12)$$

The behavior of $\mathcal{B}(\tilde{\alpha}, \Theta)$ against α and for a set of values of g is shown in Fig. 2, demonstrating the quick saturation of the Bell-CHSH function to the Cirel'son bound and the reduction (exponential with the value of the gain g) in the threshold amplitude for the violation of the inequality.

A. Effective amplification

The unbound nature of \hat{G}_j makes the transformation $|\alpha\rangle \rightarrow |\tilde{\alpha}\rangle$ implementable only probabilistically. The realization of noiseless amplification has been at the centre of an intense theoretical and experimental activity [10, 11, 17–20]. The role of noiseless amplification in quantum information processing and quantum communication has been addressed in an ample variety of ways [20–22]. For weak coherent states and small values

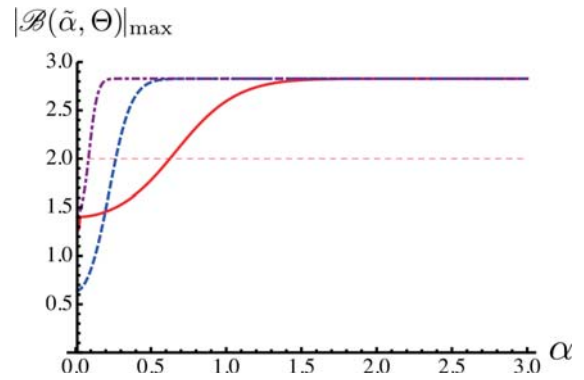


FIG. 2. Bell-CHSH function $\mathcal{B}(\tilde{\alpha}, \Theta)$, optimized over the set of rotation angles Θ , plotted against α for $g = 1$ (solid red line), $g = 2$ (blue dashed line) and $g = 3$ (purple dot-dashed line). The light straight line marks the local realistic bound.

of the gain, the amplification operator can be expanded to the first order in g as [10]

$$\hat{G}_j \simeq \hat{\mathbf{1}} + (g-1)\hat{a}_j^\dagger \hat{a}_j = (g-2)\hat{a}_j^\dagger \hat{a}_j + \hat{a}_j \hat{a}_j^\dagger. \quad (13)$$

The amplification thus results in the application of a weighted coherent superposition of the operators $\hat{a}_j^\dagger \hat{a}_j$ and $\hat{a}_j \hat{a}_j^\dagger$. Both photon-subtraction and addition operations have already been realized experimentally for arbitrary states of light [23]. A general superposition of these two operators can be experimentally engineered with a suitable configuration of stimulated parametric down-conversion and linear optics elements and with only a negligible contribution from multiphoton events [24].

A remark is due at this stage: when Eq. (13) is used together with the local operations discussed in Sec. II and dichotomized homodyne measurements, the actual ordering of the amplification and rotation stages is key to the success of the overall protocol. In particular, it takes a straightforward albeit lengthy calculation to show that, when the amplification (with $g \ll 1$) precedes the bilocal rotations, no advantage with respect to the no-amplification version of the scheme is achieved. Indeed, the state resulting from the application of the operator $\hat{U}'_A \otimes \hat{U}'_B$ [with \hat{G}_j approximated as in Eq. (13) and only the cases of successful bilateral amplification being retained] reads

$$\begin{aligned} |\psi'_f\rangle &\simeq \mathcal{N} \{ \cos[\theta_B - \theta_A] |\text{ECS}(\alpha)\rangle \\ &\quad + \sin[\theta_B - \theta_A] |\text{ECS}'(\alpha)\rangle \}, \end{aligned} \quad (14)$$

which bears no dependence on the amplification gain. Differently, we will prove in what follows that amplification following local rotations indeed results in a more advantageous resource that exhibits features similar to those of the fully amplified state in Eq. (9). We thus describe the protocol for the construction of the Bell-CHSH function resulting from the application of the \hat{U}_j 's onto $|\text{ECS}(\alpha)\rangle$ and dichotomized homodyne measurements.

The construction of the Bell-CHSH function goes along the lines described in the previous Subsection with the new correlation function [16]

$$C_{\alpha}^g(\theta_A, \theta_B, 0, 0) = \frac{e^{4\alpha^2} \nu \operatorname{Erf}[\sqrt{2}\alpha]}{(\mu_{\alpha} + \nu)^2} \left\{ 4\operatorname{Erf}[\sqrt{2}\alpha] \right. \\ \times (e^{4\alpha^2} + (1 + 8(g-1)\alpha^2) \cos[\theta_A - \theta_B]) \\ \left. + \sqrt{\frac{2}{\pi}} e^{-2\alpha^2} \alpha (g-1) (e^{4\alpha^2} + \cos[\theta_A - \theta_B]) \right\}. \quad (15)$$

While a local realistic description of the entangled coherent state in the presence of the ideal local rotations and without amplification is not possible for $\alpha \gtrsim 0.63$, for a state locally amplified by $g = 1.1$ such threshold is lowered to 0.57 [cf. inset of Fig. 3 (a)].

Further reductions of the threshold value of α can be obtained increasing the gain, still remaining within the limits of validity of the second-order expansion within which our calculations have been performed. For instance, in the main panel of Fig. 3 (a) we show the Bell function, optimised numerically over Θ , for $g = 1$ (red curve) and $g = 1.4$ (blue curve), plotted against the coherent-state amplitude α . The value of α at which the Bell-CHSH inequality is first violated when the state is locally amplified goes down to 0.43, an approximately 30% reduction in the value corresponding to no local amplification. In this case the inaccuracy due to the second order expansion in g is about 2×10^{-3} . As an example, we report the value of the optimized Bell's function without amplification for $\alpha = 0.7$ which is $B_{id}^1(0.7, \Theta_{0.7}) \simeq 2.14$, and compare it to $B_{id}^{1.4}(0.7, \Theta_{0.7}^g) \simeq 2.76$, which corresponds to $g = 1.4$. We can see that, already at $\alpha = 0.7$, the Bell's function is almost saturated.

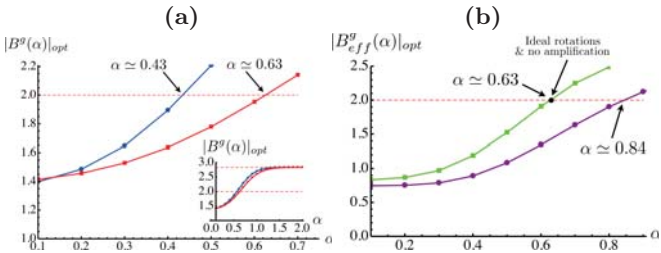


FIG. 3. (a) Bell function (optimized numerically over the set of rotation angles Θ) plotted against the coherent-state amplitude α for $g = 1.0$ (red curve) and $g = 1.4$ (blue curve). Inset: same as in the main panel but for $g = 1.0$ (red curve) and $g = 1.1$ (blue curve) and $\alpha \in [0, 2]$. Even small increases in the gain factor result in noticeable reductions of the threshold for the violation of the Bell-CHSH inequality. (b) Numerically optimized Bell's function plotted against the amplitude of the coherent states with effective rotations for $g = 1.0$ (purple curve) and $g = 1.3$ (green curve). The black point represents the value of α for which the violation occurs with ideal rotations and no amplification.

B. Effective rotations

We now replace the idealized local rotations in Eq. (2) with their physical embodiments discussed in Sec. I. We thus construct the correlation function resulting from the use of the operations approximating the local rotation operators on each mode of our system. A long albeit straightforward calculation shows that the associated joint probabilities depend on the probability amplitudes

$$C_g^{\text{eff}}(\theta_A, \theta_B, x_A, x_B) = \sum_{\gamma=\pm\alpha} \Pi_{\gamma}^g(x_A, \theta_A) \Pi_{\gamma}^g(x_B, \theta_B) \quad (16)$$

with

$$\Pi_{\pm\alpha}^g(x_j, \theta_j) = \mp \frac{i^{\delta_{\pm\alpha}^j}}{\sqrt[4]{\pi}} \left[i e^{i\theta_j} (\xi_{\chi_+}^+(x_j, \theta_j) + i \xi_{\chi_+}^-(x_j, \theta_j)) \right. \\ \left. \mp e^{-i\theta_j} (\xi_{\chi_-}^-(x_j, \theta_j) + i \xi_{\chi_-}^+(x_j, \theta_j)) \right], \\ \xi_{\chi_{\pm}}^{\pm}(x_j, \theta_j) = e^{-(x_j \mp \chi_{\pm}^j)^2} [1 + (g-1)(\pm 2\chi_{\pm}^j x_j - \chi_{\pm}^{j2})], \quad (17)$$

and $\chi_{\pm}^j = \alpha \pm i\theta_j/\alpha$. Fig. 3 (b) shows the optimized Bell-CHSH function for $g = 1.0$ (purple curve) and $g = 1.3$ (green curve). In this case, the threshold for the violation of the Bell-CHSH inequality is lowered from $\alpha = 0.84$, which is the value achieved using the effective rotations, to $\alpha = 0.63$, corresponding to the use of the ideal rotation, perfect homodyne measurements, and no amplification.

III. MULTIPARTITE NON LOCALITY TESTS USING ETS

Although one may be tempted to identify one with the other, quantum non-locality and quantum entanglement in multipartite settings are concepts which should be approached carefully. In fact, it is straightforward to real-

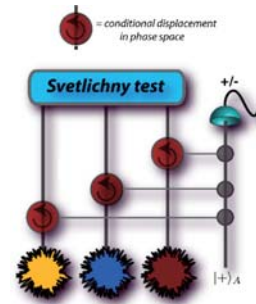


FIG. 4. Scheme for generating GHZ-like ETS. Three displaced thermal states (labelled $j = 1, 2, 3$) interact with a two-level ancilla prepared in state $|+\rangle_A = (|0\rangle_A + |1\rangle_A)/\sqrt{2}$. The interaction is ruled by the coupling Hamiltonian $\hat{H}_{Aj} = \hbar\Omega|1\rangle_A\langle 1|\hat{a}_j^\dagger\hat{a}_j$ for a time equal to π/Ω . The ancilla is finally projected onto $|\pm\rangle_A$ with $A(|+\rangle_A\langle -|_A) = 0$.

ize that the violation of an n -particle Bell's inequality by an n -particle entangled state is not sufficient to guarantee that genuine multipartite entanglement is shared by the system's elements. The non-local nature witnessed by the violation of a Bell's inequality might well be entailed simply by an entangled state involving only $m < n$ particles. In 1987, Svetlichny addressed this point by deriving an inequality, for the tripartite case, that is able to discriminate between two- and three-particle entanglement [25]. Such inequality is satisfied by restricted local realistic models allowing for a degree of two-particles non-locality.

The inequality formulated by Svetlichny reads

$$\begin{aligned} \mathcal{S}(\mathbf{a}, \mathbf{b}, \mathbf{c}) = & |\mathcal{C}(abc_1) + \mathcal{C}(ab_1c) + \mathcal{C}(a_1bc) + \mathcal{C}(abc) \\ & - \mathcal{C}(a_1b_1c) - \mathcal{C}(a_1bc_1) - \mathcal{C}(ab_1c_1) - \mathcal{C}(a_1b_1c_1)| \leq 4, \end{aligned} \quad (18)$$

where $k = a, b, c$ is a label for the party involved in the test, $\mathbf{k} = (k, k_1)$ and $\mathcal{C}(abc)$ is the statistical correlation function for measurements having outcomes a, b and c respectively. Eq. (18) states that, for any local realistic theory, the Svetlichny function $\mathcal{S}(\mathbf{a}, \mathbf{b}, \mathbf{c})$ is limited by 4. Quantum mechanics, on the other hand, predicts the existence of genuinely tripartite quantum correlated states violating such a bound. In particular, when the correlations $\mathcal{C}(abc)$ are evaluated over a tripartite GHZ state, the value $4\sqrt{2}$ is obtained for the Svetlichny function, which is the maximum achievable for any tripartite state. Such maximum violation is achieved by projecting each particle j in a GHZ state onto the eigenstates of $\cos \varphi_j \hat{\sigma}_{x,j} + \sin \varphi_j \hat{\sigma}_{y,j}$, where $\hat{\sigma}_{x,y,z}$ are the three Pauli matrices. A straightforward calculation gives the correlation function $\mathcal{C}(\theta, \phi, \mu) = \cos(\theta + \phi + \mu)$. For $\theta = \theta_1 + \pi/2 = 3\pi/4$, $\phi = -\mu_1 = \pi/2$ and $\mu = \phi_1 = 0$, we have $|\mathcal{M}| = |\mathcal{M}_1| = 2\sqrt{2}$ and $|\mathcal{S}| = 4\sqrt{2}$, which shows violation of both Svetlichny and Mermin inequality. The inequality by Svetlichny has been independently extended to the n -partite scenario in Refs. [26, 27]. Very recently, Lavoie *et al.* have experimentally demonstrated the violation of SI by a tripartite GHZ state encoded in the polarization degrees of freedom of three photons in a linear optics setup [28].

A. Generation of GHZ/W-like ETS and violation of Svetlichny inequality

We now address tripartite non-locality using ECSs and, more generally, the class of ETSs mentioned previously in this paper, used explicitly in Ref. [6, 7], and defined as $\rho_j^{\text{th}}(V, d) = \int d^2\alpha P_\alpha^{\text{th}}(V, d) |\alpha\rangle_j \langle \alpha|$, where $P_\alpha^{\text{th}}(V, d) = 2[\pi(V-1)]^{-1} e^{-\frac{2|\alpha-d|^2}{V-1}}$ is their Gaussian P function centered in d and with variance proportional to $V = 2\bar{n} + 1$ (\bar{n} is the mean thermal occupation number of the mode). In our proposal, three local parties are each provided with one mode $j = 1, 2, 3$ of a tripartite ETS that has been off-line prepared using single-mode displaced thermal states [7]. Displaced thermal states

are the building blocks for the construction of a tripartite GHZ-like ETS state, as described in the scheme of Fig. 4, which is based on conditional displacements of each of the three modes upon interaction with a two-level ancilla A having logical states $|0\rangle_A$ and $|1\rangle_A$. This is realized by enforcing the mode-ancilla coupling $\hat{H}_{Aj} = \hbar\Omega|1\rangle_A \langle 1| \hat{a}_j^\dagger \hat{a}_j$ and preparing A in $|+\rangle_A = (|0\rangle_A + |1\rangle_A)/\sqrt{2}$. Nonlinear media with free-traveling optical fields or dispersive interactions within optical/microwave cavities may be used to implement the required interactions [7, 29]. The state of A is eventually projected onto the state basis $\{|+\rangle_A, |-\rangle_A\}$ (with $A\langle -|+\rangle_A = 0$). The scheme in Fig. 4 creates the state

$$\begin{aligned} \rho_{ghz}^{(3)} = & \mathcal{N} \int d^2\alpha d^2\beta d^2\zeta P_\alpha^{\text{th}}(V, d) P_\beta^{\text{th}}(V, d) P_\zeta^{\text{th}}(V, d) \\ & \times |\text{GHZ}(\alpha, \beta, \zeta)\rangle_{123} \langle \text{GHZ}(\alpha, \beta, \zeta)| \end{aligned} \quad (19)$$

with \mathcal{N} the normalization factor, $\alpha, \beta, \zeta \in \mathbb{C}$, and the (unnormalized) GHZ-like entangled coherent state

$$|\text{GHZ}(\alpha, \beta, \zeta)\rangle_{123} = (\hat{\mathbb{1}} + \otimes_{j=1}^3 e^{i\pi \hat{a}_j^\dagger \hat{a}_j}) |\alpha, \beta, \zeta\rangle_{123}. \quad (20)$$

Both the tripartite GHZ- and W-like entangled coherent states have been shown to violate inequalities for (non-genuine) multipartite nonlocality [30]. In Ref. [31] it has been shown that Eq. (19) with an appropriate displacement amplitude can be used to violate the coherent-state version of Svetlichny inequality. Our task here is to give a clear-cut account of such results, using the set of local rotations in Eq. (2).

Following the arguments by Svetlichny illustrated above, we restrict the set of local rotations over the modes at hand to the equatorial plane in the equivalent single-qubit Bloch sphere, *i.e.* $\theta_j = \pi/2$ ($j = 1, 2, 3$) in Eq. (2), with φ_j free to change. The projections needed in order to evaluate joint probabilities and correlation functions as described in Eq. (18) are implemented by dichotomizing the outcomes of homodyne measurements performed over the three modes in $\rho_{ghz}^{(3)}$, and associating a logical +1 (−1) to a positive (negative) homodyne signal so that

$$C(\varphi_1, \varphi_2, \varphi_3) = P_{+++} - P_{---} + \mathcal{P}(P_{+--} - P_{-+-}), \quad (21)$$

where we have omitted the dependence of the above correlation function on the values of $\{\theta_j\}$, \mathcal{P} represents a permutation of the pedeces appearing in the conditional probabilities

$$P_{klp}(\varphi_1, \varphi_2, \varphi_3) = \int_{\omega_k} dx \int_{\omega_l} dy \int_{\omega_p} dz \langle x, y, z | \rho_{ghz}^{(3)'} | x, y, z \rangle, \quad (22)$$

with $k, l, p = \pm$ and $\rho_{ghz}^{(3)'} = \otimes_{j=1}^3 \hat{R}_j(\frac{\pi}{2}, \theta_j) \rho_{ghz}^{(3)} \otimes_{j=1}^3 \hat{R}_j^\dagger(\frac{\pi}{2}, \theta_j)$. In Ref. [31] it is found

$$C_{ghz}(\varphi_1, \varphi_2, \varphi_3) = \mathcal{N}_{ghz} \cos(\varphi_1 + \varphi_2 + \varphi_3) \text{Erf}^3 \left[\frac{\sqrt{2}d}{\sqrt{V}} \right] \quad (23)$$

with \mathcal{N}_{ghz} the normalisation after the local operations. When $d \gg \sqrt{V}/2$, $\text{Erf}[\sqrt{2}d/\sqrt{V}] \rightarrow 1$ and $\mathcal{N}_{ghz} \rightarrow 1$, making the correlation function identical to the one obtained for a tripartite spin-1/2 GHZ state [28].

When inefficient homodyne detectors (all with the same detection efficiency η) are considered, the correlation function is easily found from $\mathcal{C}_{ghz}(\varphi_1, \varphi_2, \varphi_3)$ with the replacements $d \rightarrow \eta d$ and $V \rightarrow 1 + \eta^2(V - 1)$ in the error function appearing in Eq. (23). So, the effect of an inefficient detector is just to slow down the saturation of the d -dependent term in the correlation function. This simply means that, for set values of V and for $\eta < 1$, a larger value of d is required to achieve the maximum allowed degree of violation of Svetlichny inequality. More in detail, for $V \gg 1$ we need to displace the local thermal states by $d_\eta \simeq d\sqrt{1 + (V\eta^2)^{-1}}$ in order for the corresponding correlation function to reach the value of $\mathcal{C}_{ghz}(\theta_1, \theta_2, \theta_3)$ corresponding to $\eta = 1$. We thus get

$$S_\eta^{ghz}(\varphi_1, \varphi_2, \varphi_3) \propto \mathcal{S}^{ghz}(\varphi_1, \varphi_2, \varphi_3) \text{Erf}^3\left[\frac{\sqrt{2}d\eta}{\sqrt{1 + \eta^2(V - 1)}}\right] \quad (24)$$

where $\mathcal{S}^{ghz}(\varphi_1, \varphi_2, \varphi_3)$ is the Svetlichny function for the ideal case of spin-1/2 particles. Fig. 5 (a) shows the Svetlichny function against V and d for $\eta = 0.1$. Maximum violations of the inequality can be observed for any value of V by choosing a sufficiently large d . The parameter d is the ‘‘knob’’ to tune in order to optimize the non-classical properties of a given state at an assigned value of the thermal spread V . Intuitively this means that the entanglement in an ETS is a delicate trade-off between the distinguishability of its state components, as measured by their mutual distance d in phase-space, and the width V of each thermal distribution. When the Gaussian probability functions defining each thermal state are so large that they overlap significantly, the state components become quasi-indistinguishable and entanglement is correspondingly destroyed. It should thus be clear that, per assigned value of V , a way to counteract such entanglement washing-out effect is to make the state components sufficiently distinguishable in phase space, which implies the increase of d .

The qualitative features discussed above do not depend on the form of the multipartite state being considered. In fact, by following arguments similar to those valid for a GHZ-like ETS state, one can easily verify that the correlation function corresponding to an ETS version of the W state, which can be generated as discussed in [30], reads (for $\eta = 1$)

$$\begin{aligned} \mathcal{C}_w(\varphi_1, \varphi_2, \varphi_3) = \mathcal{N}_w & [\cos \varphi_1 \cos \varphi_2 \cos \varphi_3 \\ & + 2 \cos(\varphi_1 + \varphi_2 + \varphi_3)] \text{Erf}^3\left[\frac{\sqrt{2}d}{\sqrt{V}}\right]. \end{aligned} \quad (25)$$

The angular part is identical to what one can find for a tripartite spin-1/2 W state $(1/\sqrt{3}) \sum_{j=1}^3 \hat{\sigma}_{x,j} |000\rangle_{123}$. This class of states violates Svetlichny inequality by $\simeq 0.355$ [32], which is achieved by projecting each party

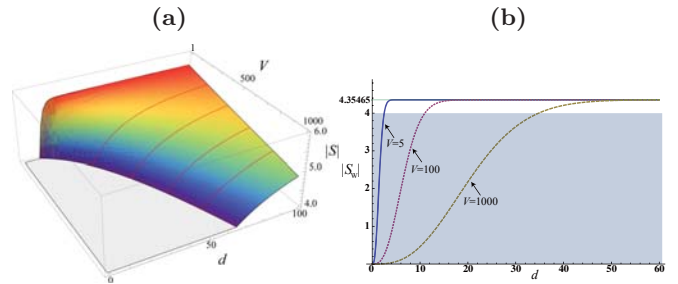


FIG. 5. (a) Violation of Svetlichny inequality by a tripartite GHZ-like ETS under effective rotations and inefficient homodyne detection (efficiency $\eta = 0.1$). We show the Svetlichny function against displacement d and variance V of the local thermal distributions. The floor of the plot is given by the local realistic bound of 4. For $d \gg \sqrt{V}$, the upper bound of $4\sqrt{2}$ is achieved, exactly as it would be for a pure GHZ state of three spin-1/2 particles under sharp measurements. (b) Svetlichny function for a tripartite W-like ETS at various values of V . The local realistic bound is 4 (shaded region of the plot). The maximum achieved violation of Svetlichny inequality, reached at large values of d , is quantitatively the same as in the spin-1/2 case.

onto the eigenstates of $\cos \varphi_j \hat{\sigma}_{z,j} + \sin \varphi_j \hat{\sigma}_{x,j}$. In our formalism, this is equivalent to applying the local rotations $\hat{R}_j(2 \arctan[(\cos \varphi_j - 1)/\sin \varphi_j], 0)$ to each mode and perform dichotomic homodyne measurements as described above. The corresponding Svetlichny function S_W is shown in Fig. 5 (b) for several values of V and $\eta = 1$. Evidently, a large enough ratio d/\sqrt{V} makes a W-like ETS state violate the tripartite Svetlichny inequality up to the maximum degree allowed to the spin-1/2 counterpart of such states. The inclusion of detection inefficiency and the corresponding results are perfectly analogous to what was discussed regarding the GHZ-like ETS case.

IV. KOCHEN-SPECKER INEQUALITY

In this Section, we abandon multi-mode non-locality to address the properties of an effective single-body quantum system against the constraints imposed by the assumptions of classical non-contextuality [33].

We briefly introduce and discuss the KS inequality that has been experimentally tested in Ref. [15], was assessed in Ref. [34] using ECSs, and is briefly reviewed in this paper. The inequality is constructed using nine observables, along the lines of the arguments put forward by Peres and Mermin [35, 36] to prove the incompatibility between quantum mechanics and non-contextuality. Such observables are arranged in a 3×3 array $\hat{\mathbf{A}}$, known as the Peres-Mermin square, in such a way that the entries \hat{A}_{ij} ($i, j=1, 2, 3$) in each column and row are mutually compatible and have dichotomic outcomes $\nu(\hat{A}_{ij}) = \pm 1$.

Denote the products of rows and columns as

$$\hat{R}_k = \hat{A}_{k1}\hat{A}_{k2}\hat{A}_{k3}, \quad \hat{C}_k = \hat{A}_{1k}\hat{A}_{2k}\hat{A}_{3k}, \quad (26)$$

respectively: Assuming non-contextuality implies that

$$\nu(\hat{R}_k) = \nu(\hat{A}_{k1})\nu(\hat{A}_{k2})\nu(\hat{A}_{k3}), \quad (27)$$

$$\nu(\hat{C}_k) = \nu(\hat{A}_{1k})\nu(\hat{A}_{2k})\nu(\hat{A}_{3k}). \quad (28)$$

Thus the total product becomes $\prod_{k=1}^3 \nu(\hat{R}_k)\nu(\hat{C}_k) = 1$, since any $\nu(\hat{A}_{ij})$ appears twice in the product. However, this is in contrast with the predictions of quantum mechanics, where a Peres-Mermin square can be built out of the dichotomic Pauli operators $\{\hat{\sigma}_x, \hat{\sigma}_y, \hat{\sigma}_z\}$ associated with two spin-1/2 systems as

$$\hat{A} = \begin{bmatrix} \hat{\sigma}_z^{(1)} \otimes \hat{1}^{(2)} & \hat{1}^{(1)} \otimes \hat{\sigma}_z^{(2)} & \hat{\sigma}_z^{(1)} \otimes \hat{\sigma}_z^{(2)} \\ \hat{1}^{(1)} \otimes \hat{\sigma}_x^{(2)} & \hat{\sigma}_x^{(1)} \otimes \hat{1}^{(2)} & \hat{\sigma}_x^{(1)} \otimes \hat{\sigma}_x^{(2)} \\ \hat{\sigma}_z^{(1)} \otimes \hat{\sigma}_x^{(2)} & \hat{\sigma}_x^{(1)} \otimes \hat{\sigma}_z^{(2)} & \hat{\sigma}_y^{(1)} \otimes \hat{\sigma}_y^{(2)} \end{bmatrix}. \quad (29)$$

In this case, the product of each row and column gives $\mathbb{1}$, except those of the last column that gives $-\mathbb{1}$. Hence, in this case we have the additional property of compatibility for \hat{R}_k and \hat{C}_k ($k=1,2,3$) and so, assuming non-contextuality, $\prod_{k=1}^3 \nu(\hat{R}_k)\nu(\hat{C}_k) = -1$. This witnesses the contradiction between a non-contextual assumption and the predictions of quantum mechanics. Such a conflicting outcome is formalized by the KS-like inequality [37]

$$\langle \hat{\chi}_{\text{KS}} \rangle = \langle \hat{R}_1 \rangle + \langle \hat{R}_2 \rangle + \langle \hat{R}_3 \rangle + \langle \hat{C}_1 \rangle + \langle \hat{C}_2 \rangle - \langle \hat{C}_3 \rangle \leq 4. \quad (30)$$

In Ref. [37] it has been proven that this inequality is bounded by 4 for any non-contextual hidden variable (NCHV) theory, while $\langle \hat{\chi}_{\text{KS}} \rangle = 6$ for any state of two spin-1/2 particles. Eq. (30) will be used throughout this paper.

In Ref. [34], the KS inequality was tested using a CV Werner-like class of states. These are defined as

$$\rho_w(a, p) = p |\text{ECS}(a)\rangle\langle \text{ECS}(a)| + \frac{(1-p)}{4} \mathbb{1}_{\pm\alpha} \quad (31)$$

with $\mathbb{1}_{\pm\alpha} = |\alpha, \alpha\rangle\langle \alpha, \alpha| + |\alpha, -\alpha\rangle\langle \alpha, -\alpha| + |-\alpha, \alpha\rangle\langle -\alpha, \alpha| + |-\alpha, -\alpha\rangle\langle -\alpha, -\alpha|$. State $|\text{ECS}(a)\rangle$ denotes the non-maximally entangled ECS state

$$|\text{ECS}(a)\rangle = \frac{(\sqrt{a}|\alpha, \alpha\rangle + \sqrt{1-a}|-\alpha, -\alpha\rangle)}{[1+2\sqrt{(1-a)ae^{-4|\alpha|^2}}]^{1/2}},$$

whose degree of entanglement is parameterised by $a \in [0, 1]$. For $a=0, 1$ the state is fully separable, while at $a=1/2$ and $|\alpha| \gg 1$ it approximates a maximally entangled two-qubit Bell state. The parameter $p \in [0, 1]$ accounts for the degree of mixedness of $\rho_w(a, p)$, which is a statistical mixture (a pure ECS state) for $p=0$ ($p=1$). The combined tuning of a and p gives us access to a broad range of states that can be used to test the KS inequality for a state-independent violation.

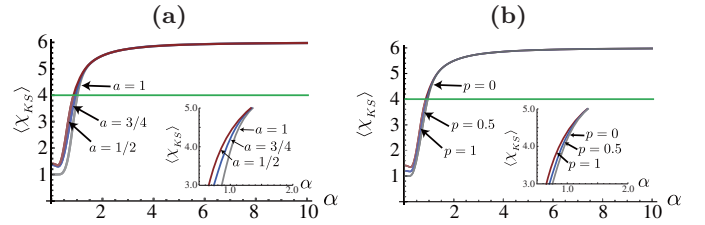


FIG. 6. (a) Violation of non-contextuality by a CV Werner state at increasing values of the amplitude $\alpha \in \mathbb{R}$. We plot three KS functions, each corresponding to $p=1$ in Eq. (31). The three curves correspond to $a=1, 3/4$ and $1/2$. Maximum violation of the non-contextual KS inequality in Eq. (30) is achieved independently of the degree of entanglement. The inset shows a magnification of the region given by $\alpha \in [0.5, 2]$. In panel (b) we have plotted the KS functions corresponding to $a=0.5$, thereby working with maximally entangled coherent states, for $p=1, 0.5$ and 0 in a CV Werner state. Maximum violation of the KS inequality is achieved, regardless of the degree of mixedness within the state. The inset shows a magnification of the region given by $\alpha \in [0.5, 2]$.

The KS function $\langle \hat{\chi}_{\text{KS}} \rangle$ for this Werner-like class of states is built from the correlators $\langle \hat{R}_i \rangle, \langle \hat{C}_i \rangle$ ($i=1, 2, 3$) as in Eq. (30). The Pauli spin-1/2 matrices $\hat{\sigma}_x, \hat{\sigma}_y$ and $\hat{\sigma}_z$ are given by $\hat{R}(0, 0), \hat{R}(0, -\pi/2)$ and $\hat{R}(\pi, 0)$, respectively. The correlator $\langle \hat{\Omega}_i \rangle$ ($\hat{\Omega} = \hat{R}, \hat{C}$ and $i=1, 2, 3$) is written as

$$\begin{aligned} \langle \hat{\Omega}_i \rangle &= (1-p) \sum_{s_{1,2}=\pm} \langle s_1\alpha, s_2\alpha | \hat{\Omega}_i | s_1\alpha, s_2\alpha \rangle / 4 \\ &+ p \langle \text{ECS}(a) | \hat{\Omega}_i | \text{ECS}(a) \rangle. \end{aligned} \quad (32)$$

The explicit form of the correlators as functions of α, p and a is too lengthy to be shown here and its components have been presented in Ref. [34].

In Fig. 6 (a) and (b), we show two significant cases of the quasi-state independence of the KS function $\langle \hat{\chi}_{\text{KS}} \rangle$ achieved in our model (for simplicity, we have taken $\alpha \in \mathbb{R}$). Panel (a) is for $p=1$ and three different values of the entanglement within the state, from full separability to maximum entanglement. On the other hand, panel (b) studies the effects that mixedness has on the behavior of $\langle \hat{\chi}_{\text{KS}} \rangle$. We set $a=0.5$, so that the CV Werner state is maximally entangled, and tune p from a fully pure state to maximum mixedness. The results show that for $\alpha < 1$, the KS function quickly grows to trespass the bound imposed by NCHV's in a narrow region around $\alpha \sim 1$. In these conditions, we observe some minor dependence of the KS function from the various states being used. The KS functions associated with resource states having larger degrees of entanglement and purity become larger than 4 for slightly smaller values of α . The situation changes as the amplitude grows, nullifying the differences highlighted above and delivering a truly state-independent KS function that quickly reaches 6, the value that is known to be achieved by $\langle \hat{\chi}_{\text{KS}} \rangle$ in the discrete-variable case and regardless of the state being

used. Although Figs. 6 (a) and (b) address only a few significant cases, we have checked that the description provided here is valid for any other choice of a and p . Ref. [34] goes significantly beyond the exemplary cases addressed here and illustrates the state-independent violation of the KS inequality for a much larger class of two-mode states.

V. CONCLUSIONS AND OUTLOOK

We have reviewed the violation of two-mode and multi-mode Bell-like inequalities by ECSs and ETSs addressing, in the former case, the potential advantages coming from the use of local noiseless amplification. We have then extended the panorama of our investigation to contextually related questions, addressing the well-known KS inequality and proving that ECS-like states can be used to prove state independent quantum contextuality. The success of the tests that we have addressed owes a lot to the nature of the local transformations that we have chosen for running both the (multipartite) Bell inequalities and the KS one described in this paper. Such studies

are interesting examples of the versatility of ECSs and reinforce the premier role that they play in the quantum information context.

ACKNOWLEDGMENTS

We acknowledge financial support from the UK EPSRC through a Career Acceleration Fellowship and the “New Directions for EPSRC Research Leaders” initiative (EP/G004759/1) as well as the National Research Foundation of Korea (NRF) grant funded by the Korean Government (No. 2010-0018295). RF and PM acknowledge project P205/12/0577, while PM also acknowledges P205/10/P319, of GA ČR. MP and FS are supported by the CNPq “Ciência sem Fronteiras” programme through the “Pesquisador Visitante Especial” initiative. MGAP acknowledges support by MIUR (FIRB LiCHIS-RBFR10YQ3H). MP thanks the UK EPSRC for a Career Acceleration Fellowship and a grant under the “New Directions for EPSRC Research Leaders” initiative (EP/G004759/1).

-
- [1] B. C. Sanders, *Journal of Physics A: Math. Theor.* **45**, 244002 (2012).
 - [2] D. Wilson, H. Jeong, and M. S. Kim, *J. Mod. Opt.* **49**, 851 (2002).
 - [3] H. Jeong, W. Son, M. S. Kim, D. Ahn, and Č. Brukner, *Phys. Rev. A* **67**, 012106 (2003).
 - [4] R. Filip, J. Rehacek, and M. Dusek, *J. Opt. B: Quantum Semiclass. Opt.* **3**, 341 (2001).
 - [5] M. Stobińska, H. Jeong, and T. C. Ralph, *Phys. Rev. A* **75**, 052105 (2007).
 - [6] H. Jeong, M. Paternostro, and T. C. Ralph, *Phys. Rev. Lett.* **102**, 060403 (2009).
 - [7] H. Jeong and T. C. Ralph, *Phys. Rev. Lett.* **97**, 100401 (2006); *Phys. Rev. A* **76**, 042103 (2007).
 - [8] J. F. Clauser, M. A. Horne, A. Shimony and R. A. Holt, *Phys. Rev. Lett.* **23**, 880 (1969).
 - [9] H. Jeong, and T. C. Ralph, *Phys. Rev. Lett.* **97**, 100401 (2006); R. Filip, M. Dusek, J. Fiurasek and L. Mista, *Phys. Rev. A* **65**, 043802 (2002).
 - [10] A. Zavatta, J. Fiurášek, and M. Bellini, *Nature Photon.* **5**, 52 (2011).
 - [11] G. Y. Xiang, T. C. Ralph, A. P. Lund, N. Walk, and G. J. Pryde, *Nature Photon.* **4**, 316 (2010).
 - [12] E. P. Specker, *Dialectica* **14**, 239 (1960).
 - [13] S. Kochen and E. P. Specker, *J. Math. Mech.* **17**, 59 (1967).
 - [14] J. S. Bell, *Rev. Mod. Phys.* **38**, 447 (1966).
 - [15] G. Kirchmair, F. Zähringer, R. Gerritsma, M. Kleinmann, O. Gühne, A. Cabello, R. Blatt, and C. F. Roos, *Nature* **460**, 494 (2009).
 - [16] G. Torlai, *et al.*, *Phys. Rev. A* (to appear, 2013); arXiv: 1301.3183v1.
 - [17] P. Marek, and R. Filip, *Phys. Rev. A* **81**, 022302 (2010); J. Fiurášek, *Phys. Rev. A* **80**, 053822 (2009).
 - [18] T. C. Ralph and A. P. Lund, in *Quantum Communication Measurement and Computing, Proceedings of 9th International Conference*, Ed. A. Lvovsky (AIP, New York 2009).
 - [19] F. Ferreyrol, M. Barbieri, R. Blandino, S. Fossier, R. Tualle-Broui, and P. Grangier, *Phys. Rev. Lett.* **104**, 123603 (2010); F. Ferreyrol, R. Blandino, M. Barbieri, R. Tualle-Broui, and P. Grangier, *Phys. Rev. A* **83**, 063801 (2011).
 - [20] M. A. Usuga, R. Ch. Müller, Ch. Wittmann, P. Marek, R. Filip, Ch. Marquardt, G. Leuchs, and U. L. Andersen, *Nature Phys* **6**, 767 (2010).
 - [21] J. B. Brask, N. Brunner, D. Cavalcanti, and A. Leverrier, *Phys. Rev. A* **85**, 042116 (2012).
 - [22] N. Gisin, S. Pironio, and N. Sangouard, *Phys. Rev. Lett.* **105**, 070501 (2010).
 - [23] A. Zavatta, S. Viciani and M. Bellini, *Phys. Rev. A* **72**, 023820 (2005); A. Zavatta, V. Parigi, M. S. Kim and M. Bellini, *New J. Phys.* **10**, 123006 (2008).
 - [24] A. Zavatta, V. Parigi, M. S. Kim, H. Jeong and M. Bellini, *Phys. Rev. Lett.* **103**, 140406 (2009).
 - [25] G. Svetlichny, *Phys. Rev. D* **35**, 3066 (1987).
 - [26] M. Seevinck and G. Svetlichny, *Phys. Rev. Lett.* **89**, 060401 (2002).
 - [27] D. Collins, N. Gisin, S. Popescu, D. Roberts, and V. Scarani, *Phys. Rev. Lett.* **88**, 170405 (2002); W. Laskowski and M. Żukowski, *Phys. Rev. A* **72**, 062112 (2005).
 - [28] J. Lavoie, R. Kaltenbaek, and K. J. Resch, *New J. Phys.* **11**, 073051 (2009).
 - [29] M. Paternostro, H. Jeong, and M.S. Kim, *Phys. Rev. A* **73**, 012338 (2006).
 - [30] H. Jeong and Nguyen Ba An, *Phys. Rev. A* **74**, 022104 (2006).

- [31] G. McKeown, F. L. Semiao, H. Jeong, and M. Paternostro, Phys. Rev. A **82**, 022315 (2010).
- [32] J. L. Cereceda, Phys. Rev. A **66**, 024102 (2002).
- [33] M. G. A. Paris, and M. Paternostro, Physics **5**, 113 (2012).
- [34] G. McKeown, M. G. A. Paris, and M. Paternostro, Phys. Rev. A **83**, 062105 (2011).
- [35] A. Peres, Phys. Lett. A **151**, 107 (1990).
- [36] N. D. Mermin, Phys. Rev. Lett. **65**, 3373 (1990).
- [37] A. Cabello, Phys. Rev. Lett. **101**, 210401 (2008).